JCTC Journal of Chemical Theory and Computation

Transferability of Nonbonded Interaction Potentials for Coarse-Grained Simulations: Benzene in Water

Alessandra Villa,[†] Christine Peter,[‡] and Nico F. A. van der Vegt*[,§]

Karolinska Institutet, SE-14183 Huddingen, Sweden, Max-Planck-Institute for Polymer Research, D-55128 Mainz, Germany, and Center of Smart Interfaces, Technische Universität Darmstadt, D-64287 Darmstadt, Germany

Received May 3, 2010

Abstract: Methods to parametrize coarse-grained simulation models for molecular fluids frequently either attempt to match the fluid structure (e.g., pair correlation functions) previously obtained with detailed atomistic models or aim at reproducing macroscopically observable thermodynamic properties. In either case, the coarse-grained models are state-point-dependent, and it is unclear to what extent the models obtained at a given state point are transferable, for example, to different compositions in the case of solution mixtures. Usually, it remains unclear as well whether structure-based potentials reproduce macroscopic thermodynamic properties and, vice versa, if thermodynamics-based potentials reproduce microscopic structural properties. In this paper, we use the Kirkwood−Buff theory of solutions in order to link local structural information and thermodynamic properties sampled with structure-based potentials. We investigate benzene/water mixtures at varying concentrations as a model hydrophobic/hydrophilic system and study the transferability of a coarse-grained model that describes the water and benzene molecules as single interaction sites. The coarse-grained model, parametrized at a high aqueous dilution of benzene, reproduces the Kirkwood−Buff integrals of mixtures obtained with the detailed-atomistic model, and it reproduces the change in the benzene chemical potential with composition up to the concentration of thermodynamic instability. The observed transferability of the potential supports the idea that hydrophobic interactions between small molecules are pairwise additive.

1. Introduction

Simulation of complex molecular systems frequently faces the challenge that time and length scales required to compare to experimentally measurable properties are hardly accessible. This is especially problematic in simulation methods that operate at a high level of resolution, for example, including atomistic or even electronic degrees of freedom. In order to bridge this time- and length-scale gap, so-called coarse-grained (CG) simulation models are being developed, where groups of atoms are treated together as larger units, thus reducing the number of degrees of freedom and speeding up the simulation. Interaction potentials for CG models are usually parametrized in such a way that properties known from experiments or from simulations at higher levels of resolution, e.g., atomistic simulations, are reproduced. In recent years, a large amount of effort has been made to investigate how far CG models are—in spite of omitting degrees of freedom—capable of reproducing both thermodynamic and structural properties of the high resolution (real) system.[1–9]

A variety of approaches has been used to develop CG nonbonded interaction potentials.[10–15] CG nonbonded potentials can be derived such that they reproduce a target structure described by a set of radial distribution functions obtained from experimental or all-atom simulation data,[16–19] or can be derived on the basis of calculation of reversible

* To whom correspondence should be addressed. E-mail: vandervegt@csi.tu-darmstadt.de.

[†] Karolinska Institutet.

[‡] Max-Planck-Institute for Polymer Research.

[§] Technische Universität Darmstadt.

10.1021/ct100228t
Published on Web 07/21/2010

work.[20–23] Alternatively, thermodynamic data can be used to parametrize the interaction between "super-atoms",[24–30] a procedure which is often based on hydrophilicity/hydrophobicity arguments.[31,32] A third approach relies on the sampling of a high-resolution system and projecting the forces onto a smaller set of coarse-grained forces.[8,33,34] It is a priori not clear how well structure-based CG potentials are suited to reproducing macroscopic thermodynamic properties and, on the other hand, how well thermodynamics-based CG models perform in terms of reproducing liquid structure. In all cases, the resulting CG potentials are state-point-dependent and their transferability to other thermodynamic states at different temperatures, compositions, etc. is limited and needs to be evaluated. This transferability, in particular to different concentrations of liquid mixtures or solutions, is of vital importance for the simulation of processes such as (bio)molecular aggregation which are characterized by spatially varying structure and fluctuating concentrations.

Recently, binary mixtures have been used as a model system to explore various aspects of the transferability of CG models obtained with different coarse-graining approaches using atomistic simulations as a reference.[1,6,8,22,35–37] Among others, Silbermann et al.[1] addressed the problem of the transferability using implicit solvent CG potentials at different ethanol/water concentrations, while Fischer et al.[6] developed implicit solvent CG models for polyoxyethylene solutions and explored the potential transferability to different chain lengths and mixture concentrations. Hess et al.[22] reported a transferable, effective two-body potential for ionic interactions in aqueous electrolytes, which could be obtained by accounting for multibody effects of the ions exerted on the dielectric behavior of the implicit solvent. In all of these models, the solvent effects are implicitly included in the solute−solute interaction potential. That makes the potentials not suitable to describing the pure liquid systems or the solute partitioning between different solvents. On the other hand, Mullinax and Noid[8] determined CG transferable potentials that are targeted at reproducing structural properties of alkane/alcohol mixtures at different concentrations. In this paper, the authors aimed at getting a single force field capable of representing solution properties at different mixtures.

In the present manuscript, we investigate to what extent a CG model can reproduce properties of both pure liquid and liquid mixtures, more precisely the liquid structure and solution thermodynamics, and to what extent a CG model can be transferred to mixtures of different concentrations of the compounds. We address these questions and use the Kirkwood−Buff (KB) theory of solution to link quantities related to the local solution structure to changes of the solute chemical potential with solution composition.[38,39] To do that, we investigate a hydrophobic/hydrophilic mixture of benzene and water. We develop two CG models based on the same atomistic description, and we apply them to different mixture conditions. In the CG models, both benzene and water molecules are treated as explicit interaction sites.

In the following sections, we will first describe how structure-based CG interaction potentials can be determined for pure fluids, mixtures, and dilute solutions. Then, we will briefly review Kirkwood−Buff theory and the relation between solution structure, KB integrals, and solution thermodynamics before we turn to the results of CG simulations of several benzene/water mixtures.

2. Nonbonded Interactions in CG Models

Structure-based coarse graining of molecular liquids relies on determining CG potentials in such a way that a predefined target function (or multiple target functions) that structurally characterizes the molecular liquid is reproduced in the CG simulation. In the present case, this means that effective two-body interaction potentials are determined to reproduce the (target/reference) radial distribution function $g_{\mathrm{ref}}(r)$ (RDF). The Boltzmann-inverted radial distribution function is the potential of mean force (PMF) between the particles:

$$V_{\mathrm{PMF}}(r) = -k_{\mathrm{B}}T \ln g_{\mathrm{ref}}(r) \equiv V_0^{\mathrm{CG}}(r) \tag{1}$$

where k_{B} denotes the Boltzmann constant and T the temperature. The PMF cannot be used directly as a two-body interaction potential in a CG model, since it incorporates multibody contributions of all the other particles in the system in a statistically averaged way. But the PMF can serve as a first guess ($V_0{}^{\mathrm{CG}}(r)$) in an iterative procedure, where these multibody contributions are eliminated and an effective two-body interaction potential is determined that reproduces the target structure. One possibility for such an iterative procedure is the so-called iterative Boltzmann inversion (IBI) method, where the initial guess potential $V_0{}^{\mathrm{CG}}$ is self-consistently refined:

$$V_{i+1}^{\mathrm{CG}}(r) = V_i^{\mathrm{CG}}(r) + k_{\mathrm{B}}T \ln\left[\frac{g_i(r)}{g_{\mathrm{ref}}(r)}\right] \tag{2}$$

Here, $g_i(r)$ denotes the RDF sampled with potential V_i^{CG} in the ith iteration. For pure fluids (where each molecule corresponds to a single CG site), the determination of the two-body potential through IBI is straightforward and converges to a unique solution (reproducing the reference radial distribution function between the molecular centers of mass) according to the Henderson theorem.[40] For liquid mixtures or solutions, or for pure fluids composed of molecules that are described by several different CG beads, the situation is more complex.[19,41,42] One reason is that in principle several RDFs need to be simultaneously reproduced, which means that several potentials, that mutually affect each other, need to be refined.[19] In the case of solutions or mixtures, one may more easily encounter convergence issues of the iteration process if the PMFs of the mixture (inverted radial distribution functions, eq 1) are a bad initial guess.

In addition, for dilute solutions, IBI becomes inefficient, because the solute−solute RDFs (solute is here referring to the low concentration component) $g_{\mathrm{ref}}(r)$ and $g_i(r)$ converge very slowly in atomistic and CG simulations. In this case, a direct determination of the PMF between two solute molecules in atomistic simulations can alternatively be obtained using free-energy calculation methods such as umbrella sampling or constraint dynamics. Because these methods are

computationally expensive, it will however be prohibitive to use them in an iterative optimization approach. Therefore, an alternative, approximate method that had been previously developed[43] is chosen here to estimate the CG solute−solute interaction potential (V_{BB}^{CG}, since in our case the solute is benzene (B) and the solvent is water (W)).

In this approach, the PMF between two solute molecules in a solvent box, V_{pmf}^{AA}, is calculated at first by all-atom (AA) simulations using constraint dynamics as described in section 4.3. The so obtained PMF incorporates thermally averaged contributions from solute degrees of freedom and from the solvent degrees of freedom; the only remaining degree of freedom is the benzene−benzene center of mass distance. Thus, this PMF cannot be directly used as a CG interaction potential if the CG model has an explicit (CG) solvent representation. To remove the solvent contributions from the PMF, a "correcting potential" is needed. To obtain this "correcting potential" (denoted as $V_{pmf,excl}^{CG}(r)$), we rerun the PMF calculation with CG potentials but exclude the direct solute−solute interaction. That means CG simulations are performed using the solvent−solvent and solute−solvent interaction potentials which had been previously obtained (for example, using the IBI method). Subtracting $V_{pmf,excl}^{CG}(r)$ from the all-atom PMF, V_{pmf}^{AA}, yields an effective two-body interaction potential that can be used as a solute−solute (i.e., benzene−benzene) potential, V_{BB}^{CG} in the CG simulations:

$$V_{BB}^{CG}(r) = V_{pmf}^{AA}(r) - V_{pmf,excl}^{CG}(r) \tag{3}$$

Note that the CG potential $V_{BB}^{CG}(r)$ does not exactly reproduce V_{pmf}^{AA}, since iteration steps in analogy to IBI—which could in principle be made—are left out since the PMF calculations are computationally expensive. Only for a neat liquid (pure B or pure W) would the above procedure yield an exact solution, as explained in more detail in ref 43. There, it is also shown for several polar and apolar solutes in aqueous solution that the so obtained approximate CG potentials reproduce the atomistic target potentials of mean force very well.

In the present study, we will investigate dilute benzene−water mixtures of various concentrations with two types of CG benzene−benzene interaction potentials. The first is derived for pure benzene using IBI, and the second is derived using the above subtraction procedure, eq 3, i.e., with potentials ideally suited for very low benzene concentrations. In both cases, the same CG water−water and water−benzene potentials are used, which are determined by IBI on the basis of atomistic simulations of pure water and a single benzene molecule in water, respectively.

3. Kirkwood−Buff Theory of Solutions

We want to address the question of transferability of CG models to various concentrations, and we want to investigate how structure-based CG models perform at reproducing certain aspects of the thermodynamic behavior of solutions. This question is of essential importance if one thinks of using such CG models for the investigation of structure formation or aggregation processes in biological systems, materials science, etc., since in these processes both structure and association thermodynamics have to be correctly represented.

To this end, we will employ the Kirkwood−Buff (KB) theory of solutions, which provides a link between the microscopic structure of the solution and its thermodynamics.[38,39] Kirkwood−Buff theory has been worked out in detail by Ben-Naim[44] and has previously been used by Smith and Weerasinghe,[45,46] as well as by others,[47−49] in parametrizations of atomistic force fields for aqueous solutions.

Usually, thermodynamic mixture properties are studied at the macroscopic level with no direct reference to molecular-scale properties. In KB theory,[44] thermodynamic properties of a solution or mixture of molecules i and j can be expressed in terms of the KB integrals, G_{ij}:

$$G_{ij} = \int_0^R [g_{ij}(r) - 1]4\pi r^2 \, dr \tag{4}$$

where $g_{ij}(r)$ is the radial distribution function between the center of mass of molecules i and j and R is a correlation distance beyond which the integrand vanishes. The quantity $\rho_j G_{ij}$, with ρ_j being the number density of molecules j, equals the change in the average number of molecules j in a spherical region of radius R caused by placing a molecule i at the center of the region. The quantity $\rho_j G_{ij}$ will in the following be referred to as the excess coordination number ΔN_{ij}:

$$\Delta N_{ij} = \rho_j \int_0^R [g_{ij}(r) - 1]4\pi r^2 \, dr \tag{5}$$

where $\rho_j = N_j/V$, N_j is the number of molecules j in the system, and V is the average volume in the (N_j, P, T) system. Since the correlation radius R typically corresponds to a few molecular diameters, the quantities G_{ij} and ΔN_{ij} are local quantities determined by the local fluid structure.

In our analysis of benzene (B)/water (W) mixtures, we use the preferential solvation parameter defined as

$$\Delta_{BW} = G_{BB} + G_{WW} - 2G_{BW} \tag{6}$$

This quantity depends on all three KB integrals in the system and provides a link with the solution thermodynamics through the KB-derived expression for the chemical potential derivative:

$$\left(\frac{\partial \mu_B}{\partial x_B}\right)_{P,T} = \frac{k_B T}{x_B(1 + \rho_B x_W \Delta_{BW})} \tag{7}$$

where μ_B is the chemical potential of compound B in the mixture at pressure P, temperature T, and composition (i.e., mole fraction) x_B. Integration of eq 7 yields

$$\mu_B(P, T, x_B) = \mu_B^p(P, T) + k_B T \ln x_B + k_B T \int_0^{x_w} \frac{\rho x'_W \Delta_{BW}}{(1 + \rho x'_B x'_W \Delta_{BW})} \, dx'_W \tag{8}$$

where $\mu_B^p(P, T)$ is the chemical potential of pure B at the same pressure P and temperature T as those of the mixture, $\rho = \rho_B + \rho_W$, and x_B and x_W are the mole fractions of B and W, respectively. When $\Delta_{BW} = 0$ at all B mole fractions between zero and x_B, we obtain $\mu_B = \mu_B^p + k_B T \ln x_B$, which is the chemical potential of B in a symmetrical ideal solution.[44] The last term on the right side of eq 8 describes

the deviation from thermodynamic ideality and is determined by the preferential solvation parameter Δ_{BW} that in turn describes the deviation of the local solution composition from the global solution composition.

Another thermodynamic quantity that will be studied is the activity coefficient of compound B, γ_B, which can be obtained from liquid/vapor equilibria according to $\gamma_B = p_B/p_B^0 x_B$. Here, ideal gas behavior of the vapor has been assumed, p_B is the equilibrium vapor pressure of component B, p_B^0 the saturation vapor pressure of pure B, and x_B is the mole fraction of B in the liquid phase. The derivative with respect to the composition x_B is given by

$$\left(\frac{\partial \ln \gamma_B}{\partial \ln x_B}\right)_{P,T} = -\frac{\rho_W x_B \Delta_{BW}}{1 + \rho_W x_B \Delta_{BW}} \quad (9)$$

Clearly, γ_B only varies with x_B, if $\Delta_{BW} \neq 0$; i.e,. the thermodynamic affinities between the solution components (B−B, W−W, and B−W) differ. Equation 9 provides a way to evaluate whether the CG potentials correctly describe the thermodynamic changes that occur in response to variations in the local solvent environment of a given molecule.

4. Computational Details

4.1. Simulations. In the atomistic simulations, the GROMOS 53a6 force field[50] was used for the benzene molecule and the SPC/E[51] model for water. All simulations were performed using the GROMACS suite of programs (version 4.0).[52,53] All of the simulations were performed in a periodic cubic box with dimensions longer than twice the cutoff distance. A cutoff distance of 1.0 nm was used for the Lennard-Jones interactions, and a long-range dispersion correction was applied for energy and pressure. The particle mesh Ewald method[54] was employed to treat Coulomb interactions, using a switching distance of 1.0 nm and a grid spacing of 0.12 nm and a Gaussian width of 0.32 nm. Constant pressure P and temperature T were maintained by coupling the system to an external bath at 1 bar and 300 K, using the Parrinello−Rahman barostat[55] and the Nose−Hoover thermostat,[56,57] respectively. The temperature coupling time was 0.5 ps. The pressure coupling time was 3 ps and the isothermal compressibility 4.5×10^{-5} bar^{-1}. In the atomistic simulations, a leapfrog integrator with a integration time step of 2 fs was used. The bond distances and the bond angle of the solvent water were constrained using the SETTLE algorithm.[58] All other bond distances were constrained using the LINCS algorithm.[59,60] In the coarse-grained simulations, a leapfrog stochastic dynamics integrator[61] was used to integrate the equations of motion. The inverse friction constant was set to 1.0 ps. In the parametrization procedure, all CG simulations were performed at constant NVT conditions at the average volume of the corresponding atomistic simulation. For the data collections, CG simulations were performed at constant pressure and temperature. Atomistic simulations were performed for 60−100 ns and coarse-grained simulation for 10−20 ns. Table 1 reports a summary of the simulated systems discussed in section 5.

4.2. Iterative Boltzmann Inversion. The IBI method was used to generate numerically tabulated potentials that reproduce the RDFs of pure liquid systems (pure benzene and pure water) or a dilute solution (one benzene molecule in water solution) at 300 K. The RDFs were calculated on the basis of the center of mass position of the each molecule. Simulations of 40, 55, and 140 ns were performed for liquid water (895 molecules), liquid benzene (2744 molecules), and a benzene/water solution (one benzene in 888 water molecules) to generate the reference radial distribution functions, $g_{ref}(r)$. In the IBI procedure, a 10 ns coarse-grained simulation was performed at each iteration. A value of $\sum(g(r) - g_{ref}(r))^2 < 0.01$ was chosen as a convergency criterion (where the summation runs over all distance bins). The pressure (with a target value of 1 atm) was included into the iteration process by applying a linear correction term to the tabulated potentials.[10]

Table 1. Summary of the Simulated Benzene (B)/Water (W) Mixture[a]

ρ_B	x_B	volume
	benzene−water mixture	
0.1	0.0019	402.36
0.2	0.0038	401.416
0.3	0.0057	400.276
0.4	0.0076	399.095
0.5	0.0095	407.766
0.6	0.0116	402.771
9.5	0.8390	423.345
	liquid benzene	
11.5	1	397.654

[a] The benzene molar concentration is denoted with ρ_B (M) and the benzene mole fraction with x_B. The atomistic average volumes (nm^3) are also reported.

4.3. Potential of Mean Force. Potentials of mean force, V_{pmf}, were calculated from n distance constraint simulations using

$$V_{pmf}(r) = \int_{r_m}^{r} \left[\langle f_c \rangle_s + \frac{2k_B T}{s}\right] ds \quad (10)$$

f_c is the constraint force, $\langle -f_c \rangle_s$ the average (mean) force exerted on the two particles separated by a fixed distance s, and r_m is the maximum distance between the center of mass of the two benzene molecules evaluated in the constraint simulations. When the distance between the two mass centers is constrained, free rotation of the solute−solute connecting vector remains possible, and larger volume elements are sampled at larger distances. This leads to an entropic contribution to the average constraint force that must be subtracted out. The second term of eq 10 takes care of this contribution. To keep the distance between the two molecules fixed, a linear constraint solver (LINCS)[59,60] was used.

Initial configurations were generated by moving the center of mass of benzene molecules apart with a speed of 0.001 nm/ps in vacuo starting from an equilibrated conformation at a distance of 0.28 nm. Configurations of 0.02 nm each were solvated and simulated. A total of 60 constraint simulations were performed. Each simulation was performed for 10 ns at the atomistic and coarse-grained levels.

5. Results

5.1. Coarse-Grained Models. In our CG models, each molecule is described through a single interaction site located

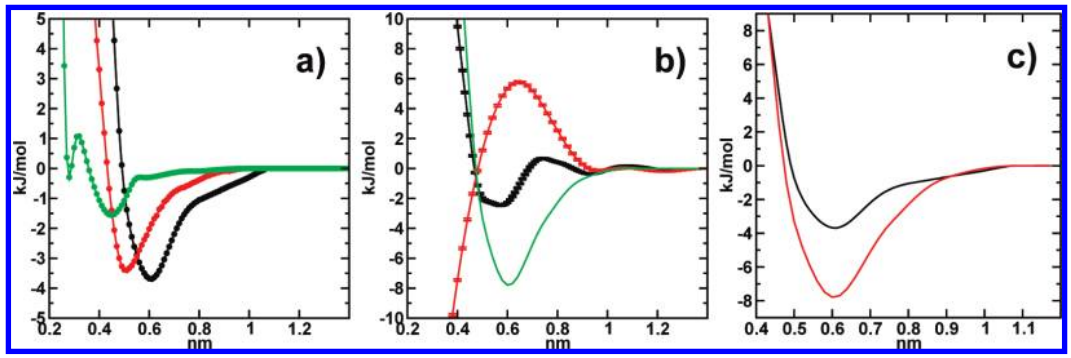

Figure 1. (a) Tabulated potentials obtained from IBI: benzene−benzene (from simulations of pure liquid benzene; black line), benzene−water (from simulations of one benzene molecule in water; red line), and water−water (from simulations of pure liquid water; green line). This model is referred to as CG(IBI). (b) Potential of mean force between two benzene molecules in aqueous solution: V_{pmf}^{AA} in black, $V_{pmf,\ excl}^{CG}$ in red, and V_{BB}^{CG} in green; this model is referred to as CG(PMF). (c) Comparison between tabulated potentials for benzene−benzene: CG(IBI) in black and CG(PMF) in red.

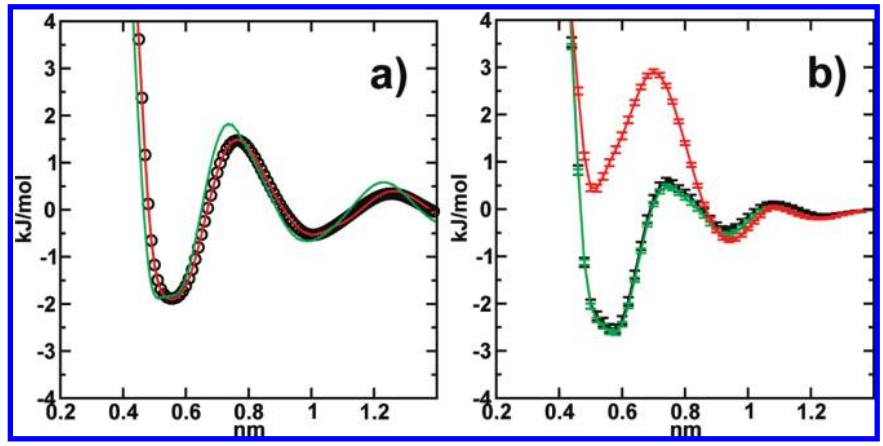

Figure 2. Potential of mean force between two benzene molecules as a function of the benzene's center of mass distance in (a) liquid benzene and (b) a water solution. Results from atomistic simulations, in black, and from CG simulations, CG(IBI) in red and CG(PMF) in green.

on the center of mass of the molecule. The potentials for solvent−solvent and solute−solvent interactions (water−water and benzene−water) were generated by IBI to reproduce the RDFs of pure liquid water and a very dilute solution (one benzene molecule in aqueous solution). The so-obtained tabulated potentials for water−water, V_{WW}^{CG}, and benzene−water, V_{BW}^{CG}, interactions are reported in Figure 1a.

Two different methods were used to determine V_{BB}^{CG} as discussed above. The first method is based on applying IBI to a pure liquid benzene system. The second method relies on benzene in water at infinite dilution where the CG nonbonded interaction potential is computed through direct determination of the potential of mean force between two benzene molecules (eq 3) with constraint dynamics. The potential obtained with the first method is shown in Figure 1a. Results from simulations performed with this potential will be labeled as CG(IBI). Figure 1b shows the PMFs together with the corresponding CG nonbonded potential obtained with the second method. Results from simulations performed with this potential will be labeled as CG(PMF). Since the subtraction method (eq 3) is only approximate, the ability of the resulting nonbonded potential to reproduce the atomistic benzene−benzene PMF in water was checked by recalculating PMFs between pairs of the solutes at the CG level. The differences between the atomistic and CG PMFs fall within the statistical errors as shown in Figure 2b.

The two CG sets of nonbonded potentials, CG(IBI) and CG(PMF), differ only in the benzene−benzene potentials. Both the benzene−benzene potentials have one minimum at 0.6 nm and a long tail that goes to zero between 1.0 and 1.1 nm, but the CG(PMF) potential shows a deeper minimum than CG(IBI) one as shown in Figure 1c.

By construction, the "pressure-corrected" CG(IBI) potentials reproduce the density of the atomistic reference of the respective pure liquids at NPT conditions.[62] In contrast to CG(IBI), the B−B interaction in the CG(PMF) model is not "pressure-corrected". At 1 atm, liquid benzene, modeled with the CG(PMF) model, has a density of 1.052 kg/L, which compares to the 0.895 kg/L obtained with the atomistic model. In dilute aqueous solutions, the effect of this is probably negligible.

5.2. Potential of Mean Force between Benzene Molecules. The two benzene−benzene CG potentials have been derived in two different environments, one in liquid benzene—CG(IBI)—and the other in a dilute benzene solution—CG(PMF). We want to see to what extent the potentials are transferable when the environment around the

benzene molecules changes (i.e., from a liquid benzene environment to a liquid water environment for the CG(IBI) model and from a liquid water environment to a liquid benzene environment for the CG(PMF) model). Figure 2 shows the PMF between two benzenes in liquid benzene and in water solution. In this figure, the atomistic results (black line) are compared with the CG(IBI) (red) and CG(PMF) (green) simulations. Figure 2a clearly shows that the CG(PMF) model reproduces the benzene−benzene PMF in liquid benzene with reasonable accuracy. We observed a tiny shift of the minima toward a shorter distance and slightly higher barriers. Figure 2b shows the PMF between two benzene molecules in water. The figure clearly shows that with the CG(IBI) model the shape of the benzene−benzene PMF deviates strongly from the atomistic reference PMF at distances smaller than 0.85 nm. The AA model predicts a global minimum at a benzene−benzene distance of around 0.5 nm, and a second minimum at 0.9 nm (corresponding to the solvent separated minimum), while the CG(IBI) PMF shows the global minimum at 0.9 nm in agreement with the second minimum of the AA potential of mean force. From the curve shown in Figure 2b, we deduce that the aggregation between benzene molecules in water solution is not favorable when the CG(IBI) model is used. Note again that with the CG(PMF) model, the calculated benzene−benzene PMF closely resembles the atomistic reference PMF.

5.3. KB Analysis of Benzene/Water Mixtures. To better understand to what extent the developed CG potentials are transferable, we simulate benzene/water mixtures at different concentrations. Atomistic and coarse-grained simulations have been performed for benzene−water mixtures at low (from 0.1 to 0.6 M) and high (9.5 M) benzene concentrations. Note that a benzene concentration of 0.5 M (40 g/L) is higher than the experimental benzene solubility in water (1.78 g/L at 298 K[63]). In the simulations presented here, benzene and water remain miscible above the experimental solubility limit. This observation reflects the fact that the GROMOS 53A6 force field underpredicts the benzene hydration free energy.[64]

Usually, thermodynamic mixture properties are studied at the macroscopic level with no direct reference to molecular-scale properties. Here, we want to compare the properties of the mixture simulated with the atomistic and CG models without losing the link between liquid structure and thermodynamics. This can be achieved by means of the Kirkwood−Buff theory of solution, as described in section 3. In Table 2, the values of the benzene−benzene (BB), benzene−water (BW), and water−water (WW) KB integrals (eq 4) for benzene/water mixtures at low benzene concentrations (from 0.1 to 0.5 M) are reported. Interestingly, G_{BB}, calculated from simulations with the atomistic and CG(PMF) models, shows a positive value, except at very low benzene concentrations in the case of the atomistic model, while the values obtained with the CG(IBI) model are all negative. A negative value of G_{BB} corresponds to a negative excess coordination number, $\rho_B G_{BB}$. This is an indication that the aggregation between benzene molecules in water solutions is not favorable, when the CG(IBI) model is used. This result is in line with the potential of mean force shown in Figure 2b.

Table 2. Kirkwood−Buff integrals, $G_{ij}(R)$, and Preferential Solvation Parameters (in cm^3/mol) for Different Benzene−Water Mixtures[a]

	x_B	G_{BB}	G_{BW}	G_{WW}	Δ_{BW}	δ_B	δ_W
AA	0.0019	−343	−77	−15	−204	−266	62
	0.0038	137	−83	−16	288	221	67
	0.0057	369	−91	−13	538	460	78
	0.0076	292	−93	−14	464	385	79
	0.0095	529	−107	−13	730	636	94
CG(IBI)	0.0019	−1014	−94	−10	−836	−920	84
	0.0038	−720	−92	−9	−545	−628	83
	0.0057	−636	−86	−8	−472	−550	78
	0.0076	−592	−80	−8	−440	−512	72
	0.0095	−585	−77	−7	−438	−508	70
CG(PMF)	0.0019	280	−107	−10	484	387	97
	0.0038	179	−107	−9	384	286	98
	0.0057	354	−117	−7	581	471	110
	0.0076	400	−121	−6	636	521	115
	0.0095	491	−129	−3	746	620	126

[a] Results from the atomistic and coarse-grained simulations. KB integrals have been obtained by averaging the $G_{ij}(R)$ over the R interval 1.4−1.8 nm.

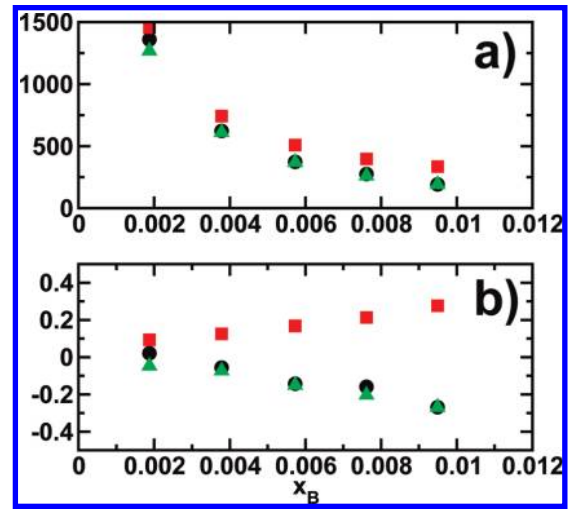

Figure 3. (a) $(\partial\mu_B/\partial x_B)_{P,T}$ (in kJ/mol) and (b) $(\partial \ln \gamma_B/\partial \ln x_B)_{P,T}$ as a function of the benzene mole fraction. Results from the simulations with the atomistic model (AA) in black, with the CG(IBI) model in red, and with the CG(PMF) model in green.

Figure 3 shows the chemical potential derivatives (eq 7) and the derivatives of the activity coefficient (eq 9) for all mixtures with a benzene concentration ranging from 0.1 to 0.5 M. The derivatives $(\partial\mu_B/\partial x_B)_{P,T}$ are all positive, indicating that the solution is thermodynamically stable at benzene concentrations ranging between 0.1 and 0.5 M. With an increasing benzene mole fraction, the derivative of the chemical potential in Figure 3a asymptotically approaches zero for all of the models. Since $(\partial\mu_B/\partial x_B)_{P,T}$ is dominated by an x_B^{-1} dependency (eq 7), we also investigated $(\partial \ln \gamma_B/\partial \ln x_B)_{P,T}$, a quantity which is more sensitive to differences in the intermolecular potentials (Figure 3b). While again the agreement between the AA and CG(PMF) models is very good at all compositions investigated, the data obtained with the CG(IBI) model increase with x_B as opposed to the data obtained with the other two models. The agreement between the CG(PMF) (corresponding to parametrization at infinite dilution) and the atomistic model indicates that the CG

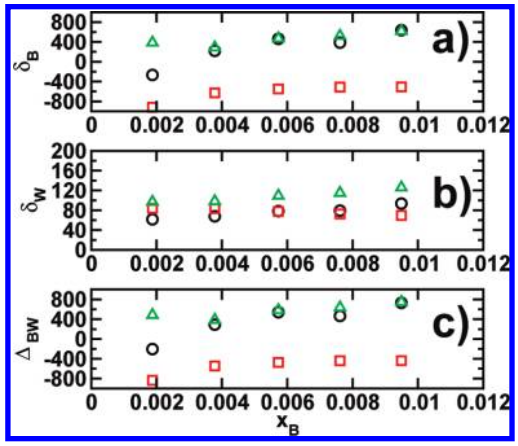

Figure 4. Preferential solvation parameters (a) $\delta_B = G_{BB} - G_{BW}$, (b) $\delta_W = G_{WW} - G_{BW}$, and (c) $\Delta_{BW} = G_{BB} + G_{WW} - 2G_{BW}$ in cm^3/mol. Results from the atomistic simulation in black, the CG(IBI) simulation in red, and the CG(PMF) simulation in green.

potentials are transferable to systems with higher benzene concentrations and reproduce the corresponding change of the benzene activity coefficient due to changes in the local solvent environment.

To further quantify how B−B and W−W affinities contribute to the observed trends in Figure 3, the preferential solvation parameter Δ_{BW} (eq 6) is written as the sum of two contributions, δ_B (characterizing the B−B affinity) and δ_W (characterizing the W−W affinity) defined as $\delta_B = G_{BB} - G_{BW}$ and $\delta_W = G_{WW} - G_{BW}$. As shown in Figure 4, we observed deviation from ideal solution behavior ($\Delta_{BW} \neq 0$) for all of the simulated mixtures, but Δ_{BW} is positive for the atomistic and CG(PMF) models while negative for the CG(IBI) model. Except for the lowest concentration, $\delta_B > \delta_W$ for the atomistic and CG(PMF) models. Hence, relative to benzene−water, the benzene−benzene affinity is stronger than the water−water affinity.

At a concentration of 0.6 M, the system starts to become unstable, as shown by the excess coordination numbers presented in Figure 5 as a function of the radius *R*. The values of the excess numbers at a long distance do not reach a plateau (as they do in a stable solution), but they diverge. With the atomistic model, the divergent trend is clearly observed for all three excess coordination numbers, and a first form of aggregation is observed as shown in the inset of Figure 5a. For the CG(PMF) model, only the benzene−water excess coordination number shows a tendency to diverge (red line in Figure 5c). The CG(IBI) model (Figure 5b) shows no indication of instability.

At a high concentration (9.5 M), all of the excess numbers obtained with the atomistic and CG(PMF) models clearly diverge, as shown in Figure 6a and c, respectively, while the excess numbers obtained with the CG(IBI) model oscillate. Phase separation between benzene and water is observed with the atomistic model after 5 ns of simulation, as shown in the inset in Figure 6a, where the two phases are easily discernible. Figure 6c clearly indicates thermodynamic instability, but phase separation cannot be easily detected visually, as shown in the inset in this figure.

6. Discussion

We have investigated two effective B−B potentials with respect to their ability to reproduce thermodynamic activities, which vary as a result of molecular association in benzene−water solutions at different mixture compositions. Because density fluctuations in aqueous solutions with hydrophobic solutes are large and strongly dependent on mixture composition, it is not a priori clear if an effective two-body potential can be found which is thermodynamically transferable, i.e., capable of describing changes in solution properties from one concentration to another. In simulations with (nonatomistic) coarse-grained models, transferability of the model cannot be guaranteed, and application of the potentials at state points away from where they were originally parametrized should always be carefully validated. Despite this obvious limitation of pair potentials used in coarse-grained models, ways exist to account for nonadditive (multibody) effects in effective pair potentials, provided that the physical nature of the nonadditivity is understood. Aqueous electrolyte solutions provide an example. For those, an implicit-solvent effective two-body potential has been previously reported that accounts for multibody contributions of the surrounding ions through their effect on the dielectric properties of the implicit solvent medium.[22]

For the present system, one may anticipate that the CG(IBI) (parametrized in the pure liquid) and CG(PMF) (parametrized at infinite dilution) potentials each are capable of describing one of the extreme cases of benzene/water mixtures. At concentrations close to instability, one might think that the CG(IBI) model should be the most appropriate choice because fluctuations are big, microscopic benzene clusters are formed, and B interacts predominantly with B. In the opposite limit, where the solution is sufficiently dilute to ignore occurrences of B−B interactions beyond two-body, we may argue that the CG(PMF) model is to be preferred. It is however not a priori clear which of the two coarse-grained potentials performs better at solution compositions located in between these two limits. A striking observation in Figure 3b is that the CG(PMF) potential is remarkably transferable over the entire range of stable-mixture compositions, while the CG(IBI) potential fails to reproduce the all-atom data of all mixtures.

A possible interpretation could be the following: Benzene aggregation in water results from hydrophobic interactions between the nonpolar benzene solutes. Small hydrophobic solutes like benzene reduce the volume of configuration space available for hydrogen bonding. The corresponding entropy loss can be minimized when solvent-separated nonpolar solutes are forced into contact. In our simulations, we use a single-site, coarse-grained water model, which, other than indirectly through the effect on the pair correlation function, does not account for hydrogen bonding. Figures 2b and 3b indeed illustrate that this water model is incapable of mediating hydrophobic benzene interactions, as evidenced by the results obtained with the CG(IBI) model, which favors benzene solvation by water rather than benzene association. The B−B interaction in this model, by construction, contains contributions of the B−B van der Waals interactions only. The CG(PMF) model, on the other hand, performs remark-

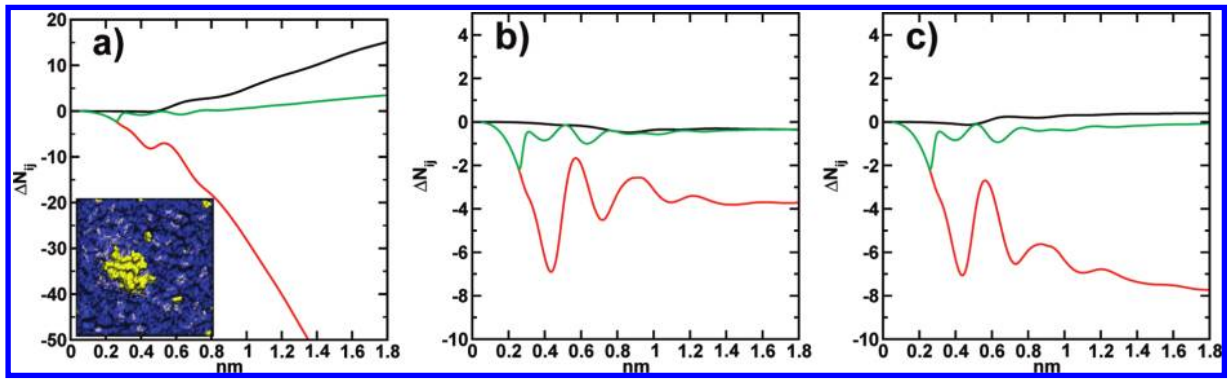

Figure 5. Benzene−benzene (black), benzene−water (red), and water−water (green) excess coordination numbers, ΔN_{ij}, as a function of the correlation distance R for a benzene−water mixture at a concentration of 0.6 M. Results from (a) atomistic, (b) CG(IBI), and (c) CG(PMF) models. The inset in part a shows an atomistic snapshot: benzene molecules in yellow and water molecules in blue.

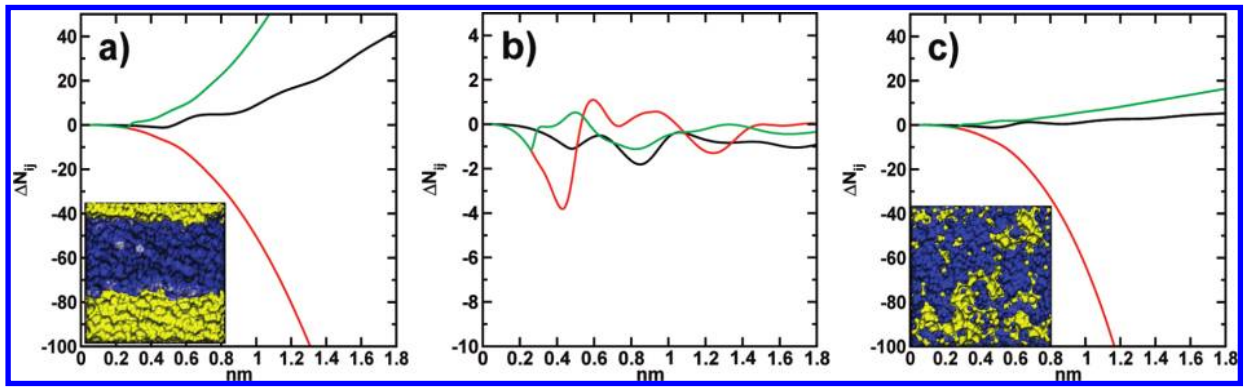

Figure 6. Benzene−benzene (black), benzene−water (red), and water−water (green) excess coordination number, ΔN_{ij}, for the benzene−water systems at a concentration of 9.5 M. Results from the (a) atomistic model, (b) CG(IBI) model, and (c) CG(PMF) model. Insets show an (a) atomistic and (c) CG(PMF) snapshot: benzene molecules in yellow and water molecules in blue.

ably well, despite the fact that it uses the same single-site water model. The CG(PMF) potential is obtained (see eq 3) by removing indirect correlations, mediated by the single-site coarse-grained water model, from the benzene−benzene pair potential of mean force in water. But since this pair potential of mean force has been obtained with a detailed atomistic model that describes water−water hydrogen bonding explicitly, the application of eq 3 yields an effective pair potential which retains the contribution of hydrophobic attraction between the solutes.

Hydrophobic association, observed with the detailed atomistic model, occurs on account of multibody correlations in the solvent (hydrogen bonding). The CG(PMF) model (eq 3) includes these multibody correlations in an *effective* pair potential, while the CG(IBI) model does not include them. The difference between these two potentials, shown in Figure 1c, indicates that the "hydrophobic contribution" has a short-range nature and a magnitude at least as large as the van der Waals interaction which the CG(IBI) model represents. This hydrophobic contribution for benzene association qualitatively compares well with the estimated strength of hydrophobic interaction between benzene solutes, as discussed by Pratt and Chandler.[65] Recent work by Wu and Prausnitz[66] on hydration free energies of short alkanes has indicated that hydrophobic interactions can be described with a pairwise additive potential; i.e., by considering the alkanes as hydrophobic associates of methylene units, it could be shown that only pairwise hydrophobic forces contribute to the free energy of hydrophobic association. The results by Wu and Prausnitz indicate that one pair potential is capable of describing hydrophobic associates with different chain lengths. In an aqueous solution of benzene, the B−B pair potential describing hydrophobic association at a low benzene concentration may therefore potentially also be used to describe hydrophobic association at larger benzene concentration. This idea is supported by the data shown in Figure 3b. This figure shows changes of the benzene activity coefficient obtained with the all-atom model that includes multibody correlations mediated by the solvent, as well as the results obtained with the CG(PMF) model in which these multibody contributions are effectively accounted for in the B−B pair potential. The observed transferability of the CG(PMF) model supports the notion that hydrophobic interactions are pairwise additive up to the concentration where the solution becomes unstable. Figure 7 shows CG and atomistic simulation snapshots of the solution at a benzene concentration just before the point where instability sets in and shows chainlike benzene clusters with up to three or four benzene molecules. The model however is not transferable to conditions where extended hydrophobic surfaces start to play a role. In such situations, where both small and large length scales are relevant, hydrophobic forces

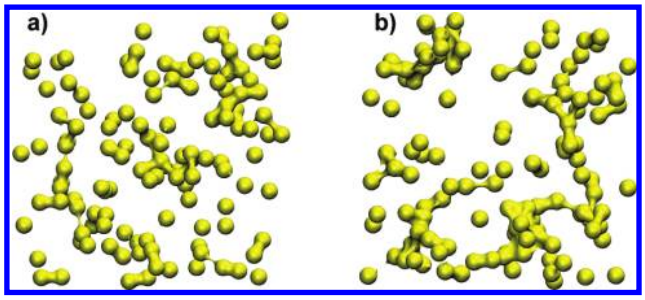

Figure 7. (a) Atomistic and (b) CG(PMF) snapshots for benzene solution at 0.5 M. For clarity, only benzene beads are shown. For the atomistic snapshots, the benzene molecules are described by the corresponding beads. The snapshots of cluster surfaces were obtained by VMD[68] using a rolling probe of 3 Å radius.

cease to be additive.[67] As evidenced by Figure 6, the CG(PMF) model does not form two well-defined phases separated by an interface under conditions where it should.

Figure 8 shows the RDFs for the AA, CG(IBI), and CG(PMF) models at two representative benzene concentrations. The WW and BW RDFs obtained with the CG(IBI) and CG(PMF) model agree very well with the AA model. The BB RDFs show some discrepancies. For example, the height of the first peak obtained with the CG(IBI) model differs clearly from that of the AA model. An important point to be made, however, is that the changes in the RDFs with concentration are fairly small. Therefore, little can be said about model transferability by investigating the RDFs. In contrast to the small differences observed in the RDFs, the KB analysis provides a much clearer picture and shows that the CG(PMF) model is perfectly transferable to other solution concentrations.

7. Conclusions

We have developed two CG models for binary mixtures of benzene and water. Both CG models are developed on the basis of atomistic reference data generated with molecular simulations, describe benzene and water molecules explicitly, but differ in the benzene−benzene interaction potential. In the CG(IBI) model, the benzene−benzene interaction potential is obtained by reproducing the structural properties of a pure liquid benzene system, while in the CG(PMF) model the parametrization has been targeted on two benzene molecules in aqueous solution at infinite dilution. Both the applied models are "structure-based" since they are derived from a benzene−benzene potential of mean force in liquid benzene or in water solution. We investigate the transferability of those CG potentials to solution compositions different from the one used in the parametrization. To this end, we use the Kirkwood−Buff theory of solutions which provides a link between the local structure of the solutions and the influence of global composition changes on chemical potentials and activity coefficients of the solution components.

We show that the CG(IBI) model is not well-suited to represent benzene in dilute aqueous solution. The model does not favor benzene aggregation as observed in detailed-atomistic simulations. We attribute this observation to the single-site CG water model, which lacks the hydrogen bonding properties needed to account for hydrophobicity, and the effective B−B pair potential, which contains only the contributions of van der Waals interactions. The CG(PMF) model correctly describes the benzene/water mixture at different benzene concentrations, as well as the structure of pure benzene solution in agreement with the atomistic model. The parametrization of this model has been based on all-atom simulations of two benzene solutes in water, which introduces hydrophobic interaction in the effective pair potential.

The Kirkwood−Buff analysis shows that the CG(PMF) potential can be used to describe benzene/water mixtures up to concentrations where the solution becomes unstable and phase separation occurs with the atomistic model. At all concentrations where the solution is stable, the agreement with the reference atomistic result is very good. At concentrations where phase separation occurs in the atomistic simulation, the solution simulated with the CG(PMF) model shows a tendency to become unstable as well, although it does not completely phase-separate, while with the CG(IBI) model the solution remains artificially stable.

The present work not only shows that carefully designed structure-based CG models are to some extent transferable

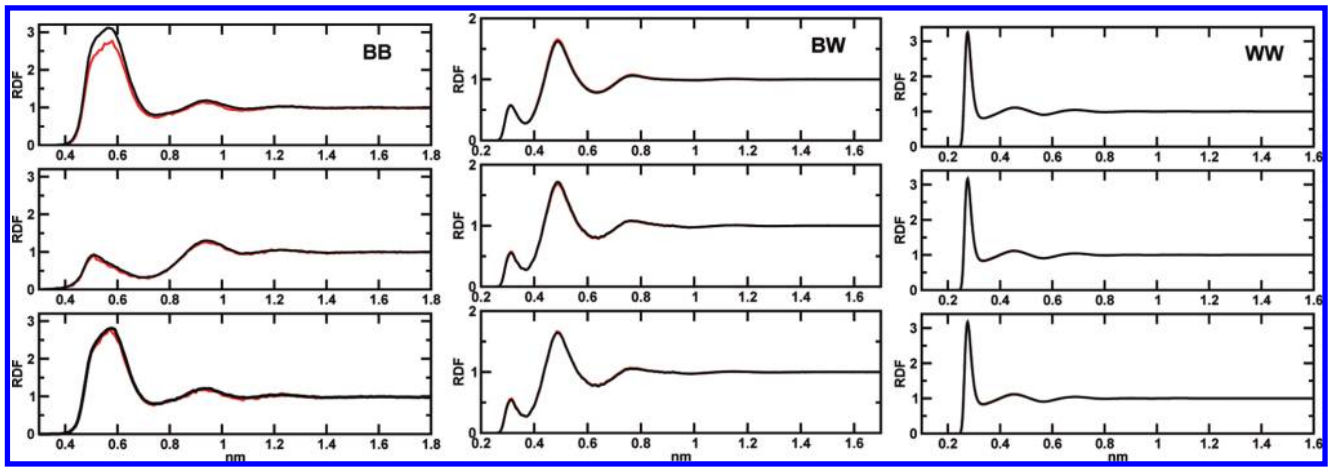

Figure 8. Molecular radial distribution function for a pair of molecules in a benzene−water mixture at different concentrations: 0.5 M (black line) and 0.2 M (red line). Results from atomistic (top), CG(IBI) (middle), and CG(PMF) (bottom) simulations.

to different concentrations, it also shows that models derived to reproduce structures of liquid mixtures or solutions are not by construction incapable of reproducing thermodynamic properties of those systems as well. By applying KB theory to our atomistic and CG simulations, we not only analyze the mixing properties of the different systems, we also illustrate in which way structural properties and thermodynamic properties of solutions are linked. KB theory provides a link between *local* solution structure and changes in the chemical potential and the activity coefficient that occur after a change in the *global* mixture composition. From a methodological perspective, KB theory, therefore, is ideally suited to analyze the transferability of CG potentials to different state points (global solution compositions). This transferability analysis works particularly well for structure-based CG potentials since in this case KB integrals of atomistic and CG simulation match at the reference state by construction.

The consistency of a CG model in terms of both structure and thermodynamics is essential if one studies biomolecular aggregation, where both structural arrangement and partitioning, hydrophobicity, or hydrophilicity are key properties. A certain level of transferability of the simulation model is also important since these processes are characterized by fluctuating and spatially varying concentrations.

Acknowledgment. We would like to thank Emiliano Brini and Jia-Wei Shen for carefully reading the manuscript. C.P. acknowledges financial support by the German Science Foundation within the Emmy Noether Programme (grant PE1625/1-1).

References

(1) Silbermann, J.; Klapp, S. H. L.; Schoen, M.; Chennamsetty, N.; Bock, H.; Gubbins, K. *J. Chem. Phys.* **2006**, *124*, 074105.

(2) Liu, P.; Izvekov, S.; Voth, G. A. *J. Phys. Chem. B* **2007**, *111*, 11566–11575.

(3) Johnson, M. E.; Head-Gordon, T.; Louis, A. A. *J. Chem. Phys.* **2007**, *126*, 144509.

(4) Qian, H.; Carbone, P.; Chen, X.; Karimi-Varzaneh, H.; Liew, C.; Muller-Plathe, F. *Macromolecules* **2008**, *41*, 9919.

(5) Allen, E. C.; Rutledge, G. C. *J. Chem. Phys.* **2008**, *128*, 154115.

(6) Fischer, J.; Paschek, D.; Geiger, A.; Sadowski, G. *J. Phys. Chem. B* **2008**, *112*, 13561–13571.

(7) Carbone, P.; Varzaneh, H. A. K.; Chen, X.; Muller-Plathe, F. *J. Chem. Phys.* **2008**, *128*, 064904.

(8) Mullinax, J.; Noid, W. *J. Chem. Phys.* **2009**, *131*, 104110.

(9) Sanghi, T.; Aluru, N. R. *J. Chem. Phys.* **2010**, *132*, 044703.

(10) Muller-Plathe, F. *ChemPhysChem* **2002**, *3*, 754–769.

(11) Tozzini, V. *Curr. Opin. Struct. Biol.* **2005**, *15*, 144–150.

(12) van der Vegt, N. F. A.; Peter, C.; Kremer, K. In *Coarse-Graining of Condensed Phase and Biomolecular Systems*; Chapman and Hall/CRC Press, Taylor and Francis Group: New York, 2008; Chapter: Structure-based coarse- and fine-graining in soft matter simulations.

(13) Murtola, T.; Bunker, A.; Vattulainen, I.; Deserno, M.; Karttunen, M. *Phys. Chem. Chem. Phys.* **2009**, *11*, 1869–1892.

(14) Peter, C.; Kremer, K. *Soft Matter* **2009**, *5*, 4357–4366.

(15) Rühle, V.; Junghans, C.; Lukyanov, A.; Kremer, K.; Andrienko, D. *J. Chem. Theory Comput.* **2009**, *5*, 3211–3223.

(16) Lyubartsev, A. P.; Laaksonen, A. *Phys. Rev. E* **1995**, *52*, 3730–3737.

(17) Soper, A. *Chem. Phys.* **1996**, *202*, 295–306.

(18) Reith, D.; Pütz, M.; Müller-Plathe, F. *J. Comput. Chem.* **2003**, *24*, 1626–1636.

(19) Peter, C.; Delle Site, L.; Kremer, K. *Soft Matter* **2008**, *4*, 859–869.

(20) McCoy, J. D.; Curro, J. C. *Macromolecules* **1998**, *31*, 9362–9368.

(21) Zacharopoulos, N.; Vergadou, N.; Theodorou, D. *J. Chem. Phys.* **2005**, *122*, 244111.

(22) Hess, B.; Holm, C.; van der Vegt, N. F. A. *Phys. Rev. Lett.* **2006**, *96*, 147801.

(23) Fritz, D.; Harmandaris, V. A.; Kremer, K.; van der Vegt, N. F. A. *Macromolecules* **2009**, *42*, 7579–7588.

(24) Shelley, J.; Shelley, M.; Reeder, R.; Bandyopadhyay, S.; Klein, M. *J. Phys. Chem. B* **2001**, *105*, 4464–4470.

(25) Nielsen, S. O.; Lopez, C. F.; Srinivas, G.; Klein, M. L. *J. Chem. Phys.* **2003**, *119*, 7043.

(26) Marrink, S. J.; de Vries, A. H.; Mark, A. E. *J. Phys. Chem. B* **2004**, *108*, 750–760.

(27) Bond, P. J.; Sansom, M. S. P. *J. Am. Chem. Soc.* **2006**, *128*, 2697–2704.

(28) Marrink, S. J.; Risselada, H. J.; Yefimov, S.; Tieleman, D. P.; de Vries, A. H. *J. Phys. Chem. B* **2007**, *111*, 7812–7824.

(29) Shinoda, W.; Devane, R.; Klein, M. *Mol. Simul.* **2007**, *33*, 27.

(30) Michel, J.; Orsi, M.; Essex, J. W. *J. Phys. Chem. B* **2008**, *112*, 657–660.

(31) Derreumaux, P.; Mousseau, N. *J. Chem. Phys.* **2007**, *126*, 025101.

(32) Brown, S.; Fawzi, N. J.; Head-Gordon, T. *Proc. Natl. Acad. Sci. U.S.A.* **2003**, *100*, 10712–10717.

(33) Izvekov, S.; Voth, G. A. *J. Phys. Chem. B* **2005**, *109*, 2469–2473.

(34) Zhou, J.; Thorpe, I. F.; Izvekov, S.; Voth, G. A. *Biophys. J.* **2007**, *92*, 4289–4303.

(35) Allen, E. C.; Rutledge, G. C. *J. Chem. Phys.* **2009**, *130*, 034904.

(36) Mognetti, B. M.; Virnau, P.; Yelash, L.; Paul, W.; Binder, K.; Mueller, M.; MacDowell, L. G. *J. Chem. Phys.* **2009**, *130*, 044101.

(37) Murtola, T.; Karttunen, M.; Vattulainen, I. *J. Chem. Phys.* **2009**, *131*, 055101.

(38) Kirkwood, J.; Buff, F. *J. Chem. Phys.* **1951**, *19*, 774–777.

(39) Ben-Naim, A.; Navarro, A. M.; Leal, J. *Phys. Chem. Chem. Phys.* **2008**, *10*, 2451–2460.

(40) Henderson, R. L. *Phys. Lett. A* **1974**, *49*, 197–198.

(41) Jain, S.; Garde, S.; Kumar, S. K. *Ind. Eng. Chem. Res.* **2006**, *45*, 5614–5618.

(42) Lyubartsev, A. P.; Mirzoev, A.; Chen, L.; Laaksonen, A. *Faraday Discuss.* **2010**, *144*, 43–56.

(43) Villa, A.; van der Vegt, N. F. A.; Peter, C. *Phys. Chem. Chem. Phys.* **2009**, *11*, 2077–2086.

(44) Ben-Naim, A. *Molecular Theory of Solutions*; Oxford Univ. Press: New York, 2006.

(45) Weerasinghe, S.; Smith, P. E. *J. Phys. Chem. B* **2003**, *107*, 3891–3898.

(46) Weerasinghe, S.; Smith, P. E. *J. Chem. Phys.* **2003**, *119*, 11342–11349.

(47) Lee, M. E.; van der Vegt, N. F. A. *J. Chem. Phys.* **2005**, *122*, 114509.

(48) Hess, B.; van der Vegt, N. F. A. *Proc. Natl. Acad. Sci. U.S.A.* **2009**, *106*, 13296–13300.

(49) Klasczyk, B.; Knecht, V. *J. Chem. Phys.* **2010**, *132*, 024109.

(50) Oostenbrink, C.; Villa, A.; Mark, A. E.; van Gunsteren, W. F. *J. Comput. Chem.* **2004**, *25*, 1656–1676.

(51) Berendsen, H. J. C.; Grigera, J. R.; Straatsma, T. P. *J. Phys. Chem.* **1987**, *91*, 6269–6271.

(52) Berendsen, H. J. C.; van der Spoel, D.; van Drunen, R. *Comput. Phys. Commun.* **1995**, *91*, 43–56.

(53) Hess, B.; Kutzner, C.; van der Spoel, D.; Lindahl, E. *J. Chem. Theory Comput.* **2008**, *4*, 435–447.

(54) Darden, T.; York, D.; Pedersen, L. *J. Chem. Phys.* **1993**, *98*, 10089–10092.

(55) Parrinello, M.; Rahman, A. *J. Appl. Phys.* **1981**, *52*, 7182–7190.

(56) Nosé, S. *Mol. Phys.* **1984**, *52*, 255–268.

(57) Hoover, W. G. *Phys. Rev. A* **1985**, *31*, 1695–1697.

(58) Miyamoto, S.; Kollman, P. A. *J. Comput. Chem.* **1992**, *13*, 952–962.

(59) Hess, B.; Bekker, H.; Berendsen, H. J. C.; Fraaije, J. G. E. M. *J. Comput. Chem.* **1997**, *18*, 1463–1472.

(60) Hess, B. *J. Chem. Theory Comput.* **2008**, *4*, 116.

(61) van Gunsteren, W. F.; Berendsen, H. J. C. *Mol. Simul.* **1988**, *1*, 173–185.

(62) Wang, H.; Junghans, C.; Kremer, K. *Eur. Phys. J.* **2009**, *28*, 221–229.

(63) *CRC Handbook of Chemistry and Physics*, 89th ed.; Lide, D., Ed.; CRC Press: Boca Raton, FL, 2008.

(64) Schravendijk, P.; van der Vegt, N. F. A. *J. Chem. Theory Comput.* **2005**, *1*, 643–652.

(65) Pratt, L. R.; Chandler, D. *J. Chem. Phys.* **1977**, *67*, 3683–3704.

(66) Wu, J.; Prausnitz, J. M. *Proc. Natl. Acad. Sci. U.S.A.* **2008**, *105*, 9512–9515.

(67) Chandler, D. *Nature* **2005**, *437*, 640–647.

(68) Humphrey, W.; Dalke, A.; Schulten, K. *J. Mol. Graphics* **1996**, *14*, 33–38.

CT100228T